¹H NMR Conformational Study on N-Terminal Nonapeptide Sequences of HIV-1 Tat Protein: A Contribution to Structure–Activity Relationships

CARMEN MRESTANI-KLAUS[a],*, ANNETT FENGLER[a], WOLFGANG BRANDT[a], JÜRGEN FAUST[a], SABINE WRENGER[b], DIRK REINHOLD[b], SIEGFRIED ANSORGE[b] and KLAUS NEUBERT[a]

[a] Department of Biochemistry and Biotechnology, Institute of Biochemistry, Martin-Luther-University Halle-Wittenberg, Halle, Germany
[b] Center for Internal Medicine, Institute of Experimental Internal Medicine, Otto-von-Guericke-University Magdeburg, Magdeburg, Germany

Abstract: On the basis of our recent results, the N-terminal sequence of HIV-1 Tat protein as a natural competitive inhibitor of dipeptidyl peptidase IV (DP IV) is supposed to interact directly with the active site of DP IV hence mediating its immunosuppressive effects via specific DP IV interactions. Of special interest is the finding that amino acid substitutions of the Tat(1–9) peptide (MDPVDPNIE) in position 5 with S-isoleucine and in position 6 with S-leucine led to peptides with strongly reduced inhibitory activity suggesting differences in the solution conformation of the three analogues. Therefore, ¹H NMR techniques in conjunction with molecular modelling have been used here to determine the solution structure of Tat(1–9), I⁵-Tat(1–9) and L⁶-Tat(1–9) and to examine the influence of amino acid exchanges on structural features of these peptides. The defined structures revealed differences in the conformations what might be the reason for different interactions of these Tat(1–9) analogues with certain amino acids of the active site of DP IV. © 1998 European Peptide Society and John Wiley & Sons, Ltd.

Keywords: HIV-1 Tat; dipeptidyl peptidase IV; ¹H NMR spectroscopy; MD calculations; structure–activity relationships

INTRODUCTION

Tat is a viral regulatory gene of the human immunodeficiency virus type 1 (HIV-1), the etiologic agent of AIDS [1,2]. Tat is essential for viral replication since its protein is a potent transactivator of the transcription of genes expressed from the HIV-1 long terminal repeat [3,4]. It has been shown that Tat is released from HIV-1-infected cells into the extracellular medium [5]. Extracellular Tat has the ability to suppress antigen as well as anti-CD3-induced activation and proliferation of human T cells [6,7]. So far, no mechanism through which Tat may

mediate this immunosuppressive activity has been proposed.

Dipeptidyl peptidase IV (DP IV) is a transmembrane serine protease and is highly expressed on T cells, but also on activated NK cells and B lymphocytes. DP IV has been shown to be identical with the T cell activation antigen CD26 [8]. DP IV/CD26 is involved in the degradation and post-translational processing of bioactive peptides. Recently, DP IV was proposed to be a co-receptor needed for HIV-1 entry into cells what is controversially discussed [8,9].

DP IV cleaves dipeptides of the sequence Xaa-Pro or Xaa-Ala from the free unsubstituted N-terminus of a peptide chain thus belonging to the group of proline-specific proteases. Interestingly, HIV-1

---

* Correspondence to: Department of Biochemistry and Biotechnology, Institute of Biochemistry, Martin-Luther-University Halle-Wittenberg, Kurt-Mothes-Str. 3, D-06120 Halle, Germany.

Tat(1–86) binds with high affinity to DP IV and inhibits the cleavage of synthetic as well as of physiological substrates suggesting the Tat immunosuppressive activity being mediated by DP IV [10,11]. In a previous paper we could show that the N-terminal sequence of Tat containing the motif Xaa-Xaa-Pro is essential for DP IV inhibition and suppression of mitogen-induced proliferation of human T cells [12]. Of special interest is our recent finding that amino acid substitutions in positions 5 and 6 of the short N-terminal nonapeptide Tat(1–9) led to peptide analogues with strongly reduced inhibitory activity compared to the parent peptide Tat(1–9) (for details see [13]). Therefore, knowledge of molecular conformation is indispensable in attempts to understand the different inhibitory activity of these peptides. In the present study, we have applied ^{1}H NMR spectroscopy and restrained molecular dynamics calculations to define the conformations of Tat(1–9), I^5-Tat(1–9) and L^6-Tat(1–9) in water solution and to examine structural requirements of the N-terminal part of Tat for the effects on DP IV activity and cell proliferation. Comparison of the conformational features and biological parameters within these peptides should help to gain insight into structure–activity relationships of short N-terminal Tat peptide sequences.

MATERIALS AND METHODS

Sample Preparation

The Tat(1–9) peptides were synthesized as previously reported [12]. The samples were prepared for NMR experiments at ≈ 6 mM concentrations in water (90% H_2O/10% D_2O).

NMR Experiments

NMR spectra were recorded on Bruker ARX500 and Varian UNITY 500 spectrometers equipped with Aspect station (Bruker) and SUN SPARC station IPX (Varian) computers, respectively. All ^{1}H spectra were measured at 303 K. Chemical shifts were calibrated with respect to d$_4$-TSPA [3-(trimethylsilyl)-3,3,2,2-tetradeuteropropionic acid Na salt]. Water suppression was achieved using presaturation during relaxation delay. The signal dispersion was such that coupling constants could be measured from the one-dimensional spectra. The dihedral angles between NH and αH were calculated from the corresponding vicinal coupling constants by the modified Karplus equation (1): $J(\theta) = A \cos^2 \theta - B \cos \theta + C$

using A, B and C values of 6.4, 1.4 and 1.9, respectively [14]. The spectra for the determination of the temperature coefficients were recorded at 303–323 K in steps of 2 K. Standard methods were used to perform the two-dimensional experiments, pulse programs being taken from the Bruker and Varian software libraries. Resonance assignments were made by analysis of the COSY [15], TOCSY [16], and ROESY [17] spectra. The TOCSY and ROESY spectra were recorded in the phase sensitive mode [18] using the TPPI [19] or States–Haberkorn–Ruben methods [20]. The TOCSY experiment employed the MLEV-17 sequence [21] for the spin-lock (mixing time, $t_m = 80$ ms). For both TOCSY and ROESY, 512 FIDs of 2 K data points, 24 scans each, were aquired. In both dimensions, the data were processed using $\pi/2$ shifted squared sinebell weighting functions. Zerofilling to 2 K was applied in ω_1.

For the ROESY spectra, a mixing time of 300 ms was used and 2.4 kHz power. NOE build-up curves are unnecessary for the calculation of distance restraints because the size of the molecules allowed us to assume that the peptides are within the motional narrowing limit ($\omega\tau_c < 1$) and that they rotate as rigid isotropic rotors [22]. The ROESY data of the Tat peptides were processed on a Silicon Graphics workstation and ROE cross-peak intensities were measured both using the TRIAD software package included in SYBYL 6.3 [23] and were classified strong, medium and weak, corresponding to interproton distances of 1.8–2.5, 1.8–3.3 and 1.8–4.0 Å, respectively.

Structure Calculations

Three-dimensional structures were generated by use of the molecular modelling program SYBYL 6.3 [23] on a Silicon Graphics workstation. The calculations were performed using the AMBER 4.1 force field [24,25]. In all cases, the N-terminus of the peptides was positively and the C-terminus negatively charged. The compounds were constructed in an extended conformation, all amide bonds were assumed to be *trans*. In the first step, the manually built nonapeptides were solvated by water using a precomputed water box of 1400 solvent molecules on average (TIP3P water model) and were then minimized to a convergence of energy gradient less than 0.0005 kcal/mol $\times$ Å. A distance independent dielectric constant of $\varepsilon = 1$ was used.

For the determination of the solution conformations, all interresidue ROEs obtained from two-dimensional ROESY spectra were included as

distance restraints for molecular dynamics simulations in water and were applied with a force constant of 32 kcal/Å. The residue-based cutoff distance for nonbonded interactions was set to 10 Å. The restrained molecular dynamics simulations in solution were carried out at 300 K over a period of 800 ps by using periodic boundary conditions for the decision of the stability of the solution conformations.

The frequency of all dihedral angles particularly the dihedral angle ϕ of all amino acid residues was analysed and compared with the experimental results based on Karplus equations. Those conformations with the highest average frequency in the simulation time that agreed with the dihedral angles ϕ derived from Karplus equations were used to generate solution conformations which were subsequently energy minimized. The stability of the solution conformations was proved by final dynamics simulations at 300 K over 800 ps without NMR restraints.

RESULTS

^{1}H NMR Shift Assignments

The one-dimensional ^{1}H NMR spectra of the three peptides in water show good signal dispersion. [1]H chemical shifts were assigned using COSY and TOCSY two-dimensional spectra to identify residue types from their side chain connectivities and ROESY experiments to obtain sequential assignments. Chemical shifts are listed in Table 1.

αH shifts for peptides and proteins are highly sensitive to structural effects [26,27] tending to occur downfield of random coil values for residues involved in β strand or extended secondary structure or upfield in regions of α helix. αH shifts for each residue of Tat(1–9), I[5]-Tat(1–9) and L[6]-Tat(1–9) were found to be close to their random coil values [27,28]. The deviations from random coil chemical shifts for the three peptides in water are illustrated in Figure 1. The large deviations of the first residues are due to the inductive effect of the N-terminal amino groups. Significant downfield shifts were observed for Asp[2] αH and Asp[5] αH in Tat(1–9) and for Asp[2] αH and Ile[5] αH in I[5]-Tat(1–9), which were likely to be due to the adjacent prolines in the sequence. Proline residues frequently give rise to an αH shift deviation of the preceding residue [29]. The downfield shift observed for Ile[8] αH in each of the three analogues may be due to a predisposition for

local structuring at this site of the molecules. Altogether, from these results it appears that all three peptides are relatively flexible, and a range of conformations are likely to exist in equilibrium with each other.

$^3J_{\alpha H-NH}$ Coupling Constants

$^3J_{\alpha H-NH}$ coupling constants were measured from one-dimensional spectra and are included in Table 2. These showed averaged values pointing to a degree of conformational flexibility about the backbone of the three peptides. In general, preferences for helical or extended conformations are indicated by low (<4 Hz) or high (>9 Hz) values, respectively, while conformational flexibility, common in small peptides, results in averaged values of 6–7 Hz. However, Dyson and Wright [30] have noted that coupling constants are often equivocal measures of folded conformations and that conformationally averaged values of 6–7 Hz can occur even if significant populations of folded forms are present. Therefore, observed values outside this range are significant, and the values between 7.1 and 7.6 Hz for Val[4], Asp[5], Asn[7] and Glu[9] in Tat(1–9) and L[6]-Tat(1–9) and for Val[4] and Glu[9] in I[5]-Tat(1–9) are consistent with the presence of some structural preference at these residues. Particularly, those values between 8.0 and 8.4 Hz measured for Ile[8] in Tat(1–9) and L[6]-Tat(1–9) as well as for both Ile[5] and Ile[8] in I[5]-Tat(1–9) may possess some propensity to form a turn or a turn-like structure.

Temperature Dependence; Amide Exchange

Changes of the NH resonances with temperature are related to their ability to participate in intra- or intermolecular hydrogen bonds [31,32]. Generally, temperature gradients exceeding 4 ppb/K are considered to be evidence for an external NH orientation, while values smaller than 2 ppb/K are indicative for intramolecular hydrogen bonding [33,34]. The temperature coefficients $-\Delta\delta/\Delta T$ of the amide proton chemical shifts are presented in Table 2. The amide NHs of Asn[7] (N[z]H, N[δ]H$_A$, N[δ]H$_B$) and Ile[8] in Tat(1–9) and L[6]-Tat(1–9) and the amide protons of Asn[7] (N[δ]H$_A$, N[δ]H$_B$) in I[5]-Tat(1–9) are relatively unaffected by changing temperature and are, therefore, likely involved in intramolecular hydrogen bonding or shielded from the surrounding solvent. All other NH proton shifts exhibit values consistent with a more external orientation.

Interestingly, upon dissolving the three analogues in purely D$_2$O at 280 K, some differentiation of NH

Table 1 ^{1}H NMR Chemical Shifts Given in ppm of Tat(1–9), I^5-Tat(1–9) and L^6-Tat(1–9) in 90% H$_2$O/10% D$_2$O at 303 K

Residue	NH	αH	βH	Others
Tat(1–9)				
Met^1	–	4.12	2.16	γCH$_2$ 2.60 εCH$_3$ 2.10
Asp^2	8.94	4.97	2.89, 2.64	–
Pro^{3a}	–	4.44	2.27, 2.03	γCH$_2$ 2.03 δCH$_2$ 3.84, 3.75
Val^4	8.16	4.03	2.04	γCH$_3$ 0.94, 0.91
Asp^5	8.45	4.97	2.95, 2.71	–
Pro^6	–	4.44	2.27, 1.98	γCH$_2$ 2.03, 1.98 δCH$_2$ 3.84
Asn^7	8.32	–^{b}	2.83, 2.74	δNH$_2$ 7.66, 6.96
Ile^8	7.87	4.20	1.91	γCH$_2$ 1.44, 1.18 γCH$_3$ 0.90 δCH$_3$ 0.87
Glu^9	8.22	4.32	2.16, 1.97	γCH$_2$ 2 44
I^5-Tat(1–9)				
Met^1	–	4.12	2.16	γCH$_2$ 2.60 εCH$_3$ 2.11
Asp^2	8.95	4.99	2.91, 2.65	–
Pro^3	–	4.44	2.28, 1.89	γCH$_2$ 2.03 δCH$_2$ 3.85, 3.73
Val^4	8.24	4.03	1.98	γCH$_3$ 0.95, 0.86
Ile^5	8.32	4.51	1.89	γCH$_2$ 1.51, 1.18 γCH$_3$ 0.95 δCH$_3$ 0.86
Pro^6	–	4.38	2.28, 1.89	γCH$_2$ 2.03 δCH$_2$ 3.90, 3.73
Asn^7	8.49	–^{c}	2.82, 2.75	δNH$_2$ 7.61, 6.91
Ile^8	8.10	4.21	1.89	γCH$_2$ 1.44, 1.18 γCH$_3$ 0.92 δCH$_3$ 0.86
Glu^9	8.32	4.33	2.16, 1.98	γCH$_2$ 2.44
L^6-Tat(1–9)				
Met^1	–	4.12	2.18	γCH$_2$ 2.59 εCH$_3$ 2.10
Asp^2	8.98	–^{c}	2.96, 2.73	–
Pro^3	–	4.44	2.29, 1.95	γCH$_2$ 2.04 δCH$_2$ 3.86, 3.76
Val^4	8.11	4.05	2.04	γCH$_3$ 0.93
Asp^5	8.46	–^{c}	2.96, 2.81	–
Leu^6	8.29	4.31	1.60	γCH 1.60 δCH$_3$ 0.91, 0.86
Asn^7	8.40	–^{c}	2.84, 2.73	δNH$_2$ 7.58, 6.90
Ile^8	7.95	4.19	1.89	γCH$_2$ 1 44, 1.16 γCH$_3$ 0.93 δCH$_3$ 0.86
Glu^9	8.34	4.40	2.18, 2.04	γCH$_2$ 2.47

^{a} Pro^3 was identified analogous to Pro^3 in L^6-Tat(1–9) and could hence be differentiated from Pro^6 in Tat(1–9).
^{b} Buried under the H$_2$O signal at 4.81 ppm.
^{c} Buried under the H$_2$O signal at 4.82 ppm.

exchange was observed. NH signals for all but the N-terminal Met^1, the Asp^2 as well as the Asn^7 (N$^\delta$H$_2$) residues remained visible for over 90 min. After 180 min only NH signals of Ile^8, and particularly Val^4, were observed in the case of both Tat(1–9) and L^6-Tat(1–9) and NH signals of Val^4, Ile^5 and Ile^8 were observed in the case of the I^5 analogue. This relatively slow exchange is highly significant for such small peptides, indicating protection of the NH from interactions with the solvent, most likely due to intramolecular hydrogen bond formation with nearby main chain or side chain carbonyls. The existence of some structural preference at these positions is, therefore, supported, although a degree

of averaging is present as the NMR data do not fit precisely with any single turn type. The results for Asp^2, Asp^5, Ile^8 and Glu^9 of Tat(1–9) and L^6-Tat(1–9) and for Asp^2, Asn^7 (N$^\alpha$H) and Glu^9 of I^5-Tat(1–9) are in agreement with the implication of the observed dependences of their chemical shifts on temperature. The amide NHs of Val^4 of all three peptides and the Ile^5 NH and Ile^8 NH of I^5-Tat(1–9) had large temperature dependences but slow exchanges. There are many cases where the implications of the temperature dependence of a peptide NH shift are not in agreement with deuterium exchange studies [35] and it may be that in the present work these amide protons, although inter-
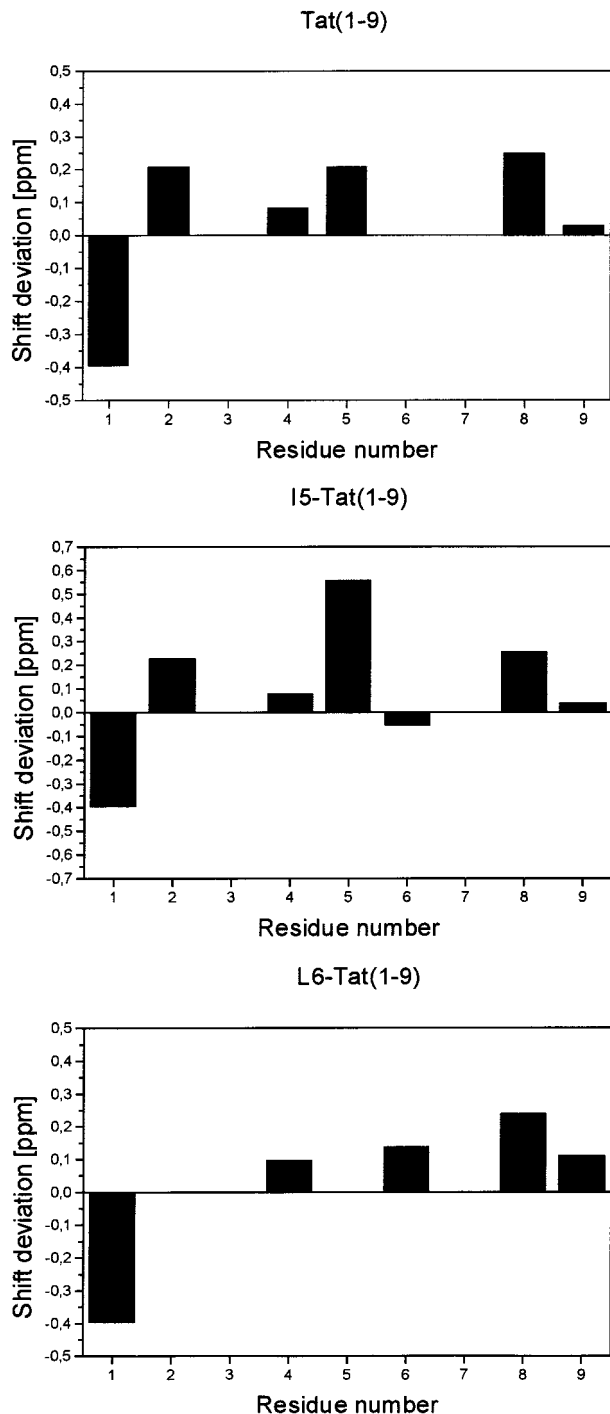
Tat(1-9)

I5-Tat(1-9)

L6-Tat(1-9)

Figure 1 Deviation of αH chemical shifts of Tat(1–9), I[5]-Tat(1–9) and L[6]-Tat(1–9) from their random coil values. These values are generally ± 0.10 ppm about the random coil chemical shifts presented by Wüthrich [27]. For Ile, Leu, and Val the random coil chemical shift values were reduced by about 0.20 ppm over those quoted by Wüthrich which was originally done by Wishart [26] in order to improve the accuracy and general applicability of these values. Asn[7] αH of all three peptides and Asp[2]/Asp[5] αH of L[6]-Tat(1–9) were buried under the H_2O signal.

nally buried, are only weakly hydrogen bonded, if at all. Furthermore, the amide NHs of Asn[7] (N$^\alpha$H) of both Tat(1–9) and L[6] analogues and Asn[7] N$^\delta$H$_A$/N$^\delta$H$_B$ of all three peptides had relatively small temperature coefficients but exchanged rapidly. The temperature coefficients of these residues may be lowered through interaction of the amide protons with charged carboxyl side chains of neighbouring residues rather than through the formation of a hydrogen bond stabilized conformation [30].

ROESY Experiments

To estimate internuclear proton–proton distances, two-dimensional ROESY (rotating frame NOE spectroscopy (NOESY)) spectra of the three peptides were obtained. The ROESY method was used instead of NOESY to avoid the problem that the cross relaxation rate is near zero for small molecules such as peptides [17,36]. None of the three peptides showed ROEs between adjacent αH protons as evidence for the existence of a *cis* peptide bond, and no chemical exchange cross peaks were observed in the TOCSY and ROESY spectra. These results indicated that the average preferred solution conformation of the three peptides is characterized by *all-trans* peptide bonds. The existence of *trans* amide bonds between Asp[2]-Pro[3] and Asp[5]/Ile[5]-Pro[6] was additionally confirmed by ROEs between Asp[2] αH and Pro[3] δH$_2$ in all three analogues and ROEs between Asp[5] αH/Ile[5] αH and Pro[6] δH$_2$ in both Tat(1–9) and I[5]-Tat(1–9). Altogether, a large number of intraresidue ROEs were obtained, about 39 for Tat(1–9), 56 for I[5]-Tat(1–9) and 47 for L[6]-Tat(1–9). Invaluable information on the structure of peptides is provided by interresidue ROEs. A summary of all interresidue ROE connectivities observed for the three peptides is given in Table 3. For all analogues, the observation of strong d$_{\alpha N}$(i, $i+1$) ROE connectivities in the absence of observable d$_{NN}$(i, $i+1$) ROEs indicates that a substantial population of the conformational ensemble of each peptide exists in 'random coil' or extended forms [30,37]. In unfolded peptides the d$_{\alpha N}$(i, i) connectivity is very much weaker than the sequential d$_{\alpha N}$(i, $i+1$) connectivity [38]. This is in agreement with the NMR data obtained by us (see Table 3 and Figure 2). d$_{\alpha N}$(i, $i+1$) ROEs between Asn[7] αH and Ile[8] NH were not observed in all three cases. However, for the I[5] and L[6] analogues weak ROEs were observed between Asn[7] NH and Ile[8] NH in both peptides and between Ile[8] NH and Glu[9] NH in I[5]-Tat(1–9) what might be a slight indication for some structural restraint in the C-terminal region of both peptides.

Table 2 Temperature Dependence of the NH Chemical Shifts Given as $-\Delta\delta/\Delta T$ (ppb/K), $^3J_{\alpha H-NH}$ Coupling Constants (Hz), Corresponding Torsion Angles ϕ (°) and Torsion Angles Observed in the Model Structure of Tat(1–9), I^5-Tat(1–9) and L^6-Tat(1–9). For Clarity, only the Karplus Angles Closest to the Observed Angles ϕ are Shown

		Met[1]	Asp[2]	Pro[3]	Val[4]	Xaa[5]	Yaa[6]	Asn[7]	Ile[8]	Glu[9]
Tat(1–9)	$-\delta\Delta/\Delta T$	—	6.77	—	8.15	8.72	—	4.65 N$^\alpha$	5.09	7.60
Xaa^5 = Asp								5.47, 5.12 N$^\delta$		
Yaa^6 = Pro	$^3J_{\alpha H-NH}$	—	6.6	—	7.6	7.3	—	7.5	8.0	7.6
	$\phi_{Karplus}$	—	−79	—	−153	−84	—	−153	−149	−88
	ϕ	—	−70	−54	−142	−66	−75	−138	−151	−86
	ψ	163	163	167	167	146	179	42	165	—
	χ_1	60	−55	−27	−62	55	30	−63	56	−168
	χ_2	175	—	36	—	—	−35	−103	168	−78
	χ_3	−174	—	−31	—	—	29	—	—	—
I^5-Tat(1–9)	$-\delta\Delta/\Delta T$	—	7.05	—	8.56	10.34	—	7.88 N$^\alpha$	7.57	7.74
Xaa^5 = Ile								5.45, 4.76 N$^\delta$		
Yaa^6 = Pro	$^3J_{\alpha H-NH}$	—	6.5	—	7.6	8.4	—	7.0	8.0	7.6
	$\phi_{Karplus}$	—	−161	—	−87	−145	—	−82	−149	−153
	ϕ	—	−139	−75	−79	−139	−58	−64	−133	−138
	ψ	131	100	171	94	163	166	136	116	—
	χ_1	−66	−179	31	−179	57	−24	176	−61	−153
	χ_2	−178	—	−35	—	—	35	−116	176	71
	χ_3	180	—	26	—	—	−33	—	—	—
L^6-Tat(1–9)	$-\delta\Delta/\Delta T$	—	7.17	—	7.73	6.79	8.51	5.58 N$^\alpha$	5.77	7.36
Xaa^5 = Asp								5.81, 4.80 N$^\delta$		
Yaa^6 = Leu	$^3J_{\alpha H-NH}$	—	6.7	—	7.1	7.6	7.0	7.6	8.1	7.5
	$\phi_{Karplus}$	—	−80	—	−83	−87	−82	−152	−149	−87
	ϕ	—	−58	−77	−72	−69	−75	−144	−138	−68
	ψ	147	153	164	166	−20	162	155	171	—
	χ_1	−170	58	32	−68	−58	−73	−179	43	62
	χ_2	176	—	−36	—	—	72	−113	62	−175
	χ_3	176	—	28	—	—	—	—	—	—

DISCUSSION

In this study we present the determination of the structure in solution of the N-terminal peptide sequences Tat(1–9), I^5-Tat(1–9) and L^6-Tat(1–9) of HIV-1 Tat protein. Although the difference of sequence between these three peptides was only one amino acid residue, they exhibited substantial different inhibitory DP IV activity [13]. By performing the NMR experiments in H$_2$O solutions we have been able to resolve and assign all of the peptide amide NH protons and most of the side chain protons. To determine the structures in solution, the proton–proton distances obtained by NMR were used as restraints in energy minimization and molecular dynamics calculations (see MATERIALS AND METHODS). Details of the structure calculations will be the subject of a separate report.

The initial structures of the three nonapeptides derived from model building were solvated by water and then subjected to conformational energy minimization, followed by molecular dynamics in the presence of distance restraints listed in Table 3. Only structurally significant interresidue distances were used, while intraresidue distances were omitted. These calculations were performed using the AMBER 4.1. force field [24,25] with explicit inclusion of solvent molecules. The solution conformations of Tat(1–9), I^5-Tat(1–9) and L^6-Tat(1–9) were derived by taking into account dihedral angles ϕ estimated from the $^3J_{\alpha H-NH}$ coupling constants and corresponding Karplus equations and by considering their frequency of occurrence in the molecular dynamics simulations. The torsion angles ϕ that occurred with the highest frequency are in close agreement with the experimentally determined val-

Table 3   Observed $d_{\alpha N}(i, i)$ and Sequential ROE Cross-Peaks in ROESY Spectra and Calculated Interproton Distances (Å) Obtained from Computer-Generated Structures

Involved protons		Tat(1–9) Xaa[5] = Asp, Yaa[6] = Pro		I[5]-Tat(1–9) Xaa[5] = Ile, Yaa[6] = Pro		L[6]-Tat(1–9) Xaa[5] = Asp, Yaa[6] = Leu	
		Cross-peak intensities[a]	r (H, H) (calculated)	Cross-peak intensities	r (H, H) (calculated)	Cross-peak intensities	r (H, H) (calculated)
Met[1]-C$^\alpha$H	Asp[2]-NH	s	2.37	s	2.15	s	2.23
Met[1]-C$^\beta$H	Asp[2]-NH	—	—	m	3.34	w	3.86
Met[1]-C$^\gamma$H	Asp[2]-NH	w	4.23	—	—	—	—
Asp[2]-NH	Asp[2]-C$^\alpha$H	—	—	—	—	w	2.95
Asp[2]-C$^\alpha$H	Pro[3]-C$^\delta$H$_2$	s	2.45	—	—	—	—
Asp[2]-C$^\alpha$H	Pro[3]-C$^\delta$H$_A$	—	—	m	2.60	s	2.38
Asp[2]-C$^\alpha$H	Pro[3]-C$^\delta$H$_B$	—	—	m	2.20	s	2.49
Asp[2]-C$^\beta$H$_A$	Pro[3]-C$^\delta$H$_B$	—	—	w	4.45	—	—
Pro[3]-C$^\alpha$H	Val[4]-NH	s	2.40	s	2.45	s	2.35
Val[4]-NH	Val[4]-C$^\alpha$H	m	3.01	m	2.92	m	2.90
Val[4]-C$^\alpha$H	Xaa[5]-NH	s	2.42	s	2.20	s	2.40
Val[4]-C$^\beta$H	Xaa[5]-NH	w	2.34	—	—	w	2.40
Val[4]-C$^\gamma$H$_3$	Xaa[5]-NH	w	4.16	—	—	w	4.32
Xaa[5]-NH	Xaa[5]-C$^\alpha$H	m	2.90	—	—	—	—
Xaa[5]-C$^\alpha$H	Yaa[6]-C$^\delta$H$_2$	s	2.21	—	—	—	—
Xaa[5]-C$^\alpha$H	Yaa[6]-C$^\delta$H$_A$	—	—	m	2.30	—	—
Xaa[5]-C$^\alpha$H	Yaa[6]-C$^\delta$H$_B$	—	—	m	2.94	—	—
Xaa[5]-C$^\alpha$H	Yaa[6]-NH	—	—	—	—	w	3.50
Yaa[6]-NH	Yaa[6]-C$^\alpha$H	—	—	—	—	m	2.90
Yaa[6]-C$^\alpha$H	Asn[7]-N$^\alpha$H	s	2.36	s	2.41	s	2.37
Yaa[6]-C$^\beta$H$_2$	Asn[7]-N$^\alpha$H	—	—	m	2.78	m	3.06
Yaa[6]-C$^\gamma$H	Asn[7]-N$^\alpha$H	—	—	—	—	w	3.87
Asn[7]-N$^\alpha$H	Ile[8]-NH	—	—	w	4.48	w	4.37
Ile[8]-NH	Ile[8]-C$^\alpha$H	m	3.00	m	2.96	m	2.94
Ile[8]-NH	Glu[9]-NH	—	—	w	4.07	—	—
Ile[8]-C$^\alpha$H	Glu[9]-NH	s	2.39	s	2.15	s	2.46
Ile[8]-C$^\beta$H	Glu[9]-NH	—	—	w	4.37	—	—
Ile[8]-C$^\gamma$H$_3$	Glu[9]-NH	w	4.25	—	—	w	4.07
Glu[9]-NH	Glu[9]-C$^\alpha$H	m	3.00	m	2.97	m	2.86

[a] s, strong; m, medium; w, weak.

ues of ϕ (Table 2). On the basis of the performed molecular dynamics simulations the frequency of the interaction of each amide proton with the solvent water as well as the frequency to form intramolecular hydrogen bonds were analysed. According to the experimental results the protons exhibiting large temperature coefficients and fast H,D exchange showed the highest frequencies in forming external hydrogen bonds to the solvent. The energetically optimized solution conformations of the three Tat derivatives which best fit the NMR data such as ROEs, torsion angles ϕ, temperature coefficients of the amide proton chemical shifts and H,D exchange experiments are presented in Figure 3. Table 3 lists the interhydrogen distances ob-

tained from the model of the solution conformations and shows good correlation with the distances calculated from the ROE data. The only exception is the experimentally obtained weak ROE between Val[4] βH and Asp[5] NH in both Tat(1–9) and L[6]-Tat(1–9) although the calculated distances indicate strong ROEs. In an attempt to change the starting conformations for a weak ROE between these protons, after rotation of χ_1 a strong ROE between Val[4] γH and Asp[5] NH was obtained resulting in energetically unfavourable conformations that were not subjected to further investigation.

The substitution of the Pro[6] amino acid residue in Tat(1–9) with Leu[6] produced some conformational changes in the backbone conformation in solution

particularly affecting torsion angles ϕ at Val[4] and ψ observed at Asp[5] and Asn[7] (Table 2, Figure 3). Thus, the strong ROE between Asp[5] αH and Pro[6] δH$_2$ in the native Tat(1–9) pointed to a torsion angle ψ at Asp[5] of about 160° whereas in L[6]-Tat(1–9) a weak ROE between Asp[5] αH and Leu[6] NH was obtained yielding $\psi = -20°$ at Asp[5]. The change of ψ at Asn[7] in Tat(1–9) of about 42 to 155° in L[6]-Tat(1–9) was confirmed by an additional ROE observed between Asn[7] NH and Ile[8] NH in the L[6] derivative.

The replacement of the Asp[5] amino acid residue in Tat(1–9) with Ile[5] led to a solution conformation that revealed even more pronounced differences in the backbone conformation. This conformation considerably differed in the ϕ angles at Asp[2], Val[4], Ile[5], Asn[7], Glu[9] and in the ψ angles at Asp[2], Val[4], Asn[7] and Ile[8] (see Table 2) compared with both Tat(1–9) and L[6]-Tat(1–9). These changed torsion angles were compatible with the experimental results. Thus, a number of ROEs observed in both Tat(1–9) and L[6]-Tat(1–9) were weakened or not observed at all whereas additional ROEs occurred in the I[5] analogue (Table 3).

In contrast to the parent peptide Tat(1–9), the amino acid residues Met[1] to Val[4] adopt an extended structure in both I[5]- and L[6]-Tat(1–9) (see Figure 3).
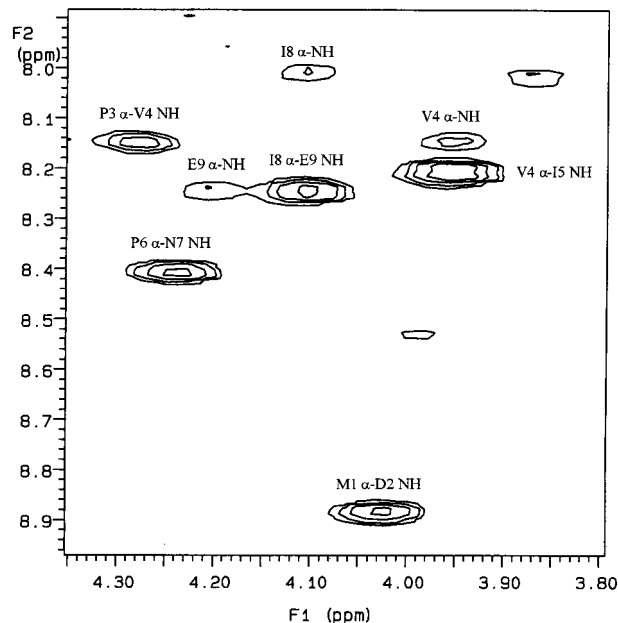

Figure 2 Portion of the two-dimensional 500-MHz ^{1}H NMR ROESY spectrum (300 ms mixing time) of I[5]-Tat(1–9) as an example illustrating d$_{\alpha N}(i, i)$ and sequential connectivities.

To investigate the question of binding properties of the three nonapeptides to DP IV the developed solution conformations of Tat(1–9), I[5]-Tat(1–9) and L[6]-Tat(1–9) were docked into the previously described model of the active site of DP IV [39]. Although no experimental indications exist the modelling studies suggest that the docking conformations of the Tat peptides to DP IV are similar to their solution conformations except small conformational alterations. While these studies the three peptides exhibited a very different docking behaviour. Thus, the native Tat(1–9) fits well into the binding pocket of the DP IV and forms several significant hydrophobic interactions as well as intermolecular hydrogen bonds with the amino acids of the enzyme active site hence explaining the high affinity and inhibitory activity of Tat(1–9) to DP IV (details will be published elsewhere). In contrast to Tat(1–9) important hydrophobic interactions of the amino acid residues of both I[5]- and L[6]-Tat(1–9) with the active site model of DP IV are weakened or completely removed likely due to their different backbone conformation what might be the reason for the relatively low inhibitory activity of the I[5] and L[6] analogues.

Taking into account that in an induced fit mechanism the L[6]-Tat(1–9) derivative may adopt a conformation similar to that of Tat(1–9) solution conformation, Pro[6] was substituted with Leu. An energy optimization of this structure forces L[6]-Tat(1–9) considerably out of the binding pocket leading to a conformation of the ligand where several interactions with the enzyme active site were weakened.

GENERAL CONSIDERATIONS

Combined use of NMR experiments and restrained molecular dynamics simulations provided sufficient information to define the solution conformations of three N-terminal nonapeptide sequences of HIV-1 Tat protein. They were all found to exist in predominantly flexible structures in water, with some indication of structural restraint at Val[4] and Ile[8] in Tat(1–9) and L[6]-Tat(1–9) and at Val[4], Ile[5] and Ile[8] in I[5]-Tat(1–9). However, no evidence for well defined secondary structure was present in all three cases. Klostermeier et al. [40] recently showed by NMR, CD and fluorescence spectroscopy that the whole N-terminal domain exhibits high flexibility in conformational studies of HIV-1 Tat protein (wild type and mutant) and of HIV-1 Tat peptide fragments. This
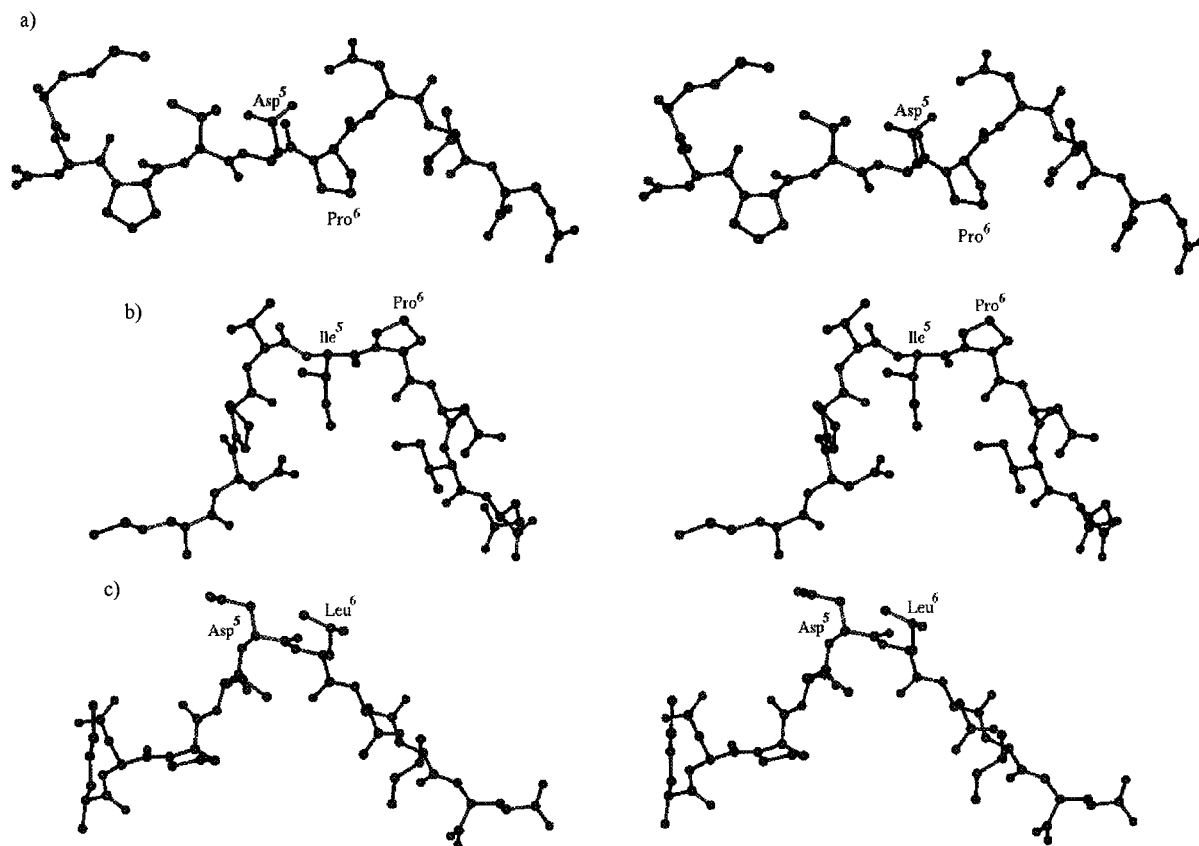
a)

b)

c)

Figure 3   Stereoview of the solution conformations of (a) Tat(1–9), (b) I^5-Tat(1–9) and (c) L^6-Tat(1–9).

correlates with our results on the structure of N-terminal sequences of HIV-1 Tat protein. The conformational differences of Tat(1–9) peptide sequences caused by amino acid substitutions in positions 5 and 6 and the nature as well as the arrangement of the side chains *per se* at these positions preventing effective binding to DP IV might both plausibly explain the lack of their inhibitory activity on DP IV compared with the wild type peptide. The results from this conformational analysis will aid us in disclosing the reason for the relatively high inhibitory activity of Tat(1–9), and possibly lead to rational designs of compounds possessing higher activity.

Acknowledgements

REFERENCES

1. F. Barre-Sinoussi, J.C. Chermann, F. Rey, M.T. Nugeyre, S. Chamaret, J. Gruest, C. Dauguet, C. Axler-Blin, F. Vezinet-Brun, C. Ronzioux, W. Rozenbaum and L. Montagnier (1983). Isolation of a T-lymphotropic retrovirus from a patient at risk for acquired immune deficiency syndrome (AIDS). *Science* **220**, 868–871.
2. R.C. Gallo, S.Z. Salahuddin, M. Popovic, G.M. Shearer, M. Kaplan, B.F. Haynes, T.J. Palker, R. Redfield, J. Oleske, B. Safai, G. White, P. Foster and P.D. Markham (1984). Frequent detection and isolation of cytopathic retroviruses (HTLV-III) from patients with AIDS and at risk for AIDS. *Science* **224**, 500–503.
3. J.G. Sodroski, C.A. Rosen, W.C. Goh and W.A. Haseltine (1985). A transcriptional activator protein

encoded by the x-lor region of the human T-cell leukemia virus. *Science* 228, 1430–1434.

4. A.I. Dayton, J.G. Sodroski, C.A. Rosen, W.C. Goh and W.A. Haseltine (1986). The trans-activator gene of the human T cell lymphotropic virus type III is required for replication. *Cell 44*, 941–947.

5. B. Ensoli, L. Buonaguro, G. Barillari, V. Fiorelli, R. Gendelman, R.A. Morgan, P. Wingfield and R.C. Gallo (1993). Release, uptake, and effects of extracellular human immunodeficiency virus type 1 Tat protein on cell growth and viral transactivation. *J. Virol. 67*, 277–287.

6. R.P. Viscidi, K. Mayur, HM. Lederman and A.D. Frankel (1989). Inhibition of antigen-induced lymphocyte proliferation by Tat-protein from HIV-1. *Science 246*, 1606–1608.

7. M. Subramanyam, W.G. Gutheil, W.W. Bachovchin and B.T. Huber (1993). Mechanism of HIV-1 Tat induced inhibition of antigen-specific T-cell responsiveness. *J. Immunol. 150*, 2544–2553.

8. B. Fleischer (1994). CD26: A surface protease involved in T-cell activation. *Immunol. Today 15*, 180–184.

9. C. Callebaut, B. Krust, E. Jacotot and A.G. Hovanessian (1993). T-cell activation antigen, CD26, as a cofactor for entry of HIV in CD4$^+$ cells. *Science 262*, 2045–2050.

10. W.G. Gutheil, M. Subramanyam, G.R. Flentke, D.G. Sanford, E. Munoz, B.T. Huber and W.W. Bachovchin (1994). Human immunodeficiency virus 1 Tat binds to dipeptidyl aminopeptidase IV (CD26): A possible mechanism for Tat's immunosuppressive activity. *Proc. Natl. Acad. Sci. USA 91*, 6594–6598.

11. D. Reinhold, S. Wrenger, U. Bank, F. Bühling, T. Hoffmann, K. Neubert, M. Kraft, R. Frank and S. Ansorge (1996). CD26 mediates the action of HIV-1 Tat protein on DNA synthesis and cytokine production in U937 cells. *Immunobiology 195*, 119–128.

12. S. Wrenger, D. Reinhold, T. Hoffmann, M. Kraft, R. Frank, J. Faust, K. Neubert and S. Ansorge (1996). The N-terminal X-X-Pro sequence of the HIV-1 Tat protein is important for the inhibition of dipeptidyl peptidase IV (DP IV/CD26) and the suppression of mitogen-induced proliferation of human T cells. *FEBS Lett. 383*, 145–149.

13. S. Wrenger, T. Hoffmann, J. Faust, C. Mrestani-Klaus, W. Brandt, K. Neubert, M. Kraft, S. Olek, R. Frank, S. Ansorge and D. Reinhold (1997). The N-terminal structure of HIV-1 Tat is required for suppression of CD26-dependent T cell growth. *J. Biol. Chem. 272*, 30283–30288.

14. A. Pardi, M. Billeter and K. Wüthrich (1984). Calibration of the angular dependence of the amide proton-C$^{\alpha}$ proton coupling constants, $^3J_{HN\alpha}$, in a globular protein. Use of $^3J_{HN\alpha}$ for identification of helical secondary structure. *J. Mol. Biol. 180*, 741–751.

15. W.P. Aue, E. Bartholdi and R.R. Ernst (1976). Two-dimensional spectroscopy. Application to Nuclear Magnetic Resonance. *J. Chem. Phys. 64*, 2229–2246.

16. L. Braunschweiler and R.R. Ernst (1983). Coherence transfer by isotropic mixing. Application to proton correlation spectroscopy. *J. Magn. Reson. 53*, 521–528.

17. A.A. Bothner-By, R.L. Stephens, J. Lee, C.D. Warren and R.W. Jeanloz (1984). Structure determination of a tetrasaccharide: Transient Nuclear Overhauser effects in the rotating frame. *J. Am. Chem. Soc. 106*, 811–813.

18. L. Müller and R.R. Ernst (1979). Coherence transfer in the rotating frame. Application to heteronuclear cross-correlation spectroscopy. *Mol. Phys. 38*, 963–992.

19. D. Marion and K. Wüthrich (1983). Application of phase sensitive two-dimensional correlated spectroscopy (COSY) for measurements of ^1H-^1H spin-spin coupling constants in proteins. *Biochem. Biophys. Res. Commun. 113*, 967–974.

20. D.J. States, R.A. Haberkorn and D.J. Ruben (1982). A two-dimensional Nuclear Overhauser experiment with pure absorption phase in four quadrants. *J. Magn. Reson. 48*, 286–292.

21. A. Bax and D.G. Davis (1985). MLEV-17-based two-dimensional homonuclear magnetization transfer spectroscopy. *J. Magn. Reson. 65*, 355–360.

22. D. Neuhaus and M. Williamson: *The Nuclear Overhauser Effect in Structural and Conformational Analysis*, p. 103–140, VCH Publishers Inc., Weinheim 1989.

23. TRIPOS Associates, Inc., 1699 S. Hanley Road, St. Louis, Missouri 63144-2913, 1996.

24. S.J. Weiner, P.A. Kollmann, D.A. Case, U.C. Singh, C. Ghio, G. Alagano, S. Profeta, Jr and P. Weiner (1984). A new force field for molecular mechanical simulation of nucleic acids and proteins. *J. Am. Chem. Soc. 106*, 765–784.

25. S.J. Weiner, P.A. Kollmann, D.T. Nguyen and D.A. Case (1986). An all atom force field for simulations of proteins and nucleic acids. *J. Comput. Chem. 7*, 230–252.

26. D.S. Wishart, B.D. Sykes, and F.M. Richards (1991). Relationship between Nuclear Magnetic Resonance chemical shift and protein secondary structure. *J. Mol. Biol. 222*, 311–333.

27. D.S. Wishart, B.D. Sykes and F.M. Richards (1992). The chemical shift index: A fast and simple method for the assignment of protein secondary structure through NMR spectroscopy. *Biochemistry 31*, 1647–1651.

28. K. Wüthrich: *NMR of Proteins and Nucleic Acids*, p. 14–19, Wiley, New York 1996.

29. O.W. Howarth and D.M.J. Lilley (1978). Carbon-13-NMR of peptides and proteins. *Prog. NMR Spectr. 12*, 1–40.

30. H.J. Dyson and P.E. Wright (1991). Defining solution conformations of small linear peptides. *Annu. Rev. Biophys. Biophys. Chem. 20*, 519–538.

31. D.W. Urry, M. Ohnishi and R. Walter (1970). Secondary structure of the cyclic moiety of the peptide hormone oxytocin and its deamino analog. *Proc. Natl. Acad. Sci. USA 66*, 111–116.

32. D.A. Torchia, S.C.K. Wong, C.M. Deber and E.R. Blout (1972). Cyclic peptides. III. Solution conformations of cyclo (serylprolylglycylserylprolylglycyl) from Nuclear Magnetic Resonance. *J. Am. Chem. Soc. 94*, 616–620.

33. Y.A. Bara, A. Friedrich, H. Kessler and M. Molter (1978). ^{1}H NMR investigation of the conformation of cyclo (-Phe$_3$-Gly$_2$-). *Chem. Ber. 111*, 1045–1057.

34. H. Kessler, W. Bermel, A. Müller and K.-H. Pook. Modern Nuclear Magnetic Resonance spectroscopy of peptides, in: *The Peptides 1985*, S. Udenfriend, J. Meienhofer and V.J. Hruby, Eds, p. 437–473, Academic Press, Orlando, FL 1985.

35. O. Jardetzky and G.C.K. Roberts: *NMR in Molecular Biology*, p. 166, Academic Press, New York 1981.

36. A. Bax and D.G. Davis (1985). Practical aspects of two-dimensional transverse NOE spectroscopy. *J. Magn. Reson. 63*, 207–213.

37. H.J. Dyson, M. Rance, R.A. Houghten, P.E. Wright and R.A. Lerner (1988). Folding of immunogenic peptide fragments of proteins in water solution. II. The nascent helix. *J. Mol. Biol. 201*, 201–217.

38. H.J. Dyson, M. Rance, R.A. Houghten, R.A. Lerner and P.E. Wright (1988). Folding of immunogenic peptide fragments of proteins in water solution. I. Sequence requirements for the formation of a reverse turn. *J. Mol. Biol. 201*, 161–200.

39. W. Brandt, T. Lehmann, I. Thondorf, I. Born, M. Schutkowski, J.-U. Rahfeld, K. Neubert and A. Barth (1995). A model of the active site of dipeptidyl peptidase IV predicted by comparative molecular field analysis and molecular modelling simulations. *Int. J. Peptide Protein Res. 46*, 494–507.

40. D. Klostermeier, P. Bayer, M. Kraft, R.W. Frank and P. Rösch (1997). Spectroscopic investigations of HIV-1 trans-activator and related peptides in aqueous solutions. *Biophys. Chem. 63*, 87–96.